

# XMM-Newton & INTEGRAL broad-band study of the luminous quasar 4C04.42: clues on a bulk Compton feature?

Alessandra De Rosa, Pietro Ubertini (IASF-INAF, Roma), Loredana Bassani (IASF-INAF, Bologna),  
On behalf of the INTEGRAL AGN/survey TEAM

Flat Spectrum Radio Quasar (FSRQ) are considered the most luminous class of Blazar, with harder spectra associated to higher luminosity objects (Fossati et al. 1998). The Spectral Energy Distribution of FSRQ exhibits two main peaks, one between the IR and soft X frequencies and the other in the gamma-ray regime: the low energy component is due to the Synchrotron radiation of relativistic electrons in the jet, while the high energy component is due to Inverse Compton (IC) of the same electrons with a photon field (Ghisellini et al. 1998). It is also believed that in FSRQ the IC is due to Compton scattering of photons external to the jet (external Compton radiation EC), probably produced in the accretion disk and reprocessed by the BLR and/or the dusty torus. Other competitive processes (Dermer et al. 1993) can contribute to the high energy component, like IC from photons produced by Synchrotron (self-Synchrotron radiation, SSC). In several QSOs up to  $z=4$  a flattening in the soft X-ray band ( $E < 2$  keV observer frame), has been observed (Yuan et al. 2006, Fiore et al. 1998, Cappi et al. 1997) and a clear trend of  $N_H$  vs  $z$  has been measured indicating a cosmic evolution effect, which seems to be strongest at redshifts around 2. The origin of the observed behaviour is not clear yet. Possible hypotheses are intrinsic cold/ionized absorption or intrinsic break of the continuum. Another intriguing feature is the steepening of the continuum or excess counts at low energies observed in a few sources only (Kataoka et al. 2007, Sambruna et al. 2006), the origin of this behaviour is still unclear. Proposed scenarios involve bulk Compton motion or disk emission similar to that observed in radio-quiet sources. Particularly intriguing is the association of this feature with bulk Compton scattering of UV-external photons reprocessed in Broad Lines Region with "cold" electrons. Under reasonable conditions this component may give an observable feature strikingly similar to that observed (Celotti et al. 2006). 4C04.42 is a FSRQ (radio loudness parameter  $R=S(5\text{GHz})/S(4400 \text{ \AA}) \sim 1000$ ). It was detected above 20 keV by INTEGRAL (Bird et al. 2007) with a flux  $(7.6 \pm 1.5) \times 10^{-12} \text{ erg cm}^{-2} \text{ s}^{-1}$  and  $(18.8 \pm 2.8) \times 10^{-12} \text{ erg cm}^{-2} \text{ s}^{-1}$  in 20-40 keV and 40-100 keV respectively. It was successively observed by XMM-Newton for  $\sim 10$  ks. In this poster we present for the first time the broad-band analysis of this FSRQ in 0.2-200 keV through non simultaneous data of XMM-Newton and INTEGRAL (De Rosa et al. 2008).

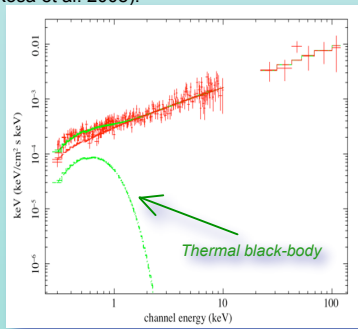


Fig. 2. Broad-band spectrum.

## Broad-band spectral analysis

The 2-200 keV best fit absorbed power-law extrapolated in 0.3-2 keV fails to reproduce the broad-band spectrum (Fig. 1). Main residuals are at the low energies strongly suggesting the presence of an excess below 2 keV (observer frame). To fit the broad-band combined spectrum XMM-Newton and INTEGRAL and to account of this emission component at the low energies we try different models: a thermal black body (in Fig. 2), a multi temperature disk emission, a broken power-law, a Compton reflection and a partial covering absorber. In Table 1 we report the best fit parameters of each of them.

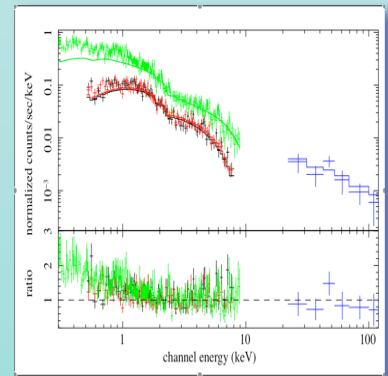


Fig. 1. 2-200 keV best fit power-law extrapolated below 2 keV

Table 1. Broad-band spectral models - best fit parameters

$^1C_{\text{Integral}}$	$\chi^2/\text{dof}$	$^2p_{\text{null}}$	$\Gamma$	$^2F_{\text{obs}}(0.1-2 \text{ keV})$ ( $10^{-12} \text{ erg cm}^{-2} \text{ s}^{-1}$ )	$^2F_{\text{obs}}(2-10 \text{ keV})$ ( $10^{-12} \text{ erg cm}^{-2} \text{ s}^{-1}$ )	$^2F_{\text{obs}}(20-100 \text{ keV})$ ( $10^{-12} \text{ erg cm}^{-2} \text{ s}^{-1}$ )	param
constant phabs zpowerlw							
1 frozen	507/411	0.0008	$1.46 \pm 0.02$	1.0	2.2	7.5	-
$2.2 \pm 0.6$	496/410	0.002	$1.47^{+0.01}_{-0.02}$	1.0	2.1	7.3	-
constant phabs zpowerlw zbb							
1 frozen	383/364	0.232	$1.28^{+0.02}_{-0.04}$	0.98	2.5	13	$0.15^{+0.02}_{-0.02}$
$1.7^{+0.3}_{-0.3}$	383/363	0.229	$1.30^{+0.04}_{-0.03}$	0.99	2.5	13.	$0.15^{+0.02}_{-0.02}$
constant phabs zpowerlw diskbb							
1 frozen	373/364	0.363	$1.22^{+0.06}_{-0.09}$	1.0	2.5	15	$0.25^{+0.04}_{-0.04}$
$0.97^{+0.04}_{-0.03}$	373/363	0.349	$1.22^{+0.09}_{-0.08}$	1	2.5	15	$0.26^{+0.04}_{-0.04}$
constant phabs brokenpowerlw							
1 frozen	365/364	0.476	$1.58^{+0.05}_{-0.07}$	1.0	2.5	16.	$2.1^{+0.4}_{-0.3}$
$0.9^{+0.3}_{-0.3}$	364/363	0.470	$1.19^{+0.05}_{-0.05}$	1.0	2.6	17	$2.2^{+0.4}_{-0.4}$
			$1.17^{+0.09}_{-0.10}$				
constant phabs zbb pexrav							
1 frozen	382/363	0.233	$1.33^{+0.09}_{-0.08}$	1.0	2.6	14	$0.25^{+0.02}_{-0.24}$
$1.1^{+0.4}_{-0.3}$	382/362	0.224	$1.33^{+0.07}_{-0.08}$	1.0	2.5	14	<0.6
constant phabs zpowerlw zpcfabs							
1 frozen	381/364	0.261	$1.56^{+0.05}_{-0.05}$	1.0	2.6	9.5	$76^{+21}_{-20} / 0.46^{+0.08}_{-0.08}$
$1.7^{+0.5}_{-0.5}$	375/363	0.320	$1.57 \pm 0.04$	1.0	2.6	8.8	$70^{+26}_{-19} / 0.45^{+0.08}_{-0.08}$

## The Spectral Energy Distribution

The simplest model to reproduce the not simultaneous SED of 4C04.42 (in Fig. 3) is that of an emitting blob of radius  $R$  moving with a bulk velocity of  $\beta c$  (with  $\beta = ((\Gamma^2 - 1)/\Gamma)^{1/2}$ , with  $\Gamma$  the Lorentz factor) in a magnetic field with intensity of 2 Gauss. The SSC+EC components are plotted separately with solid and dashed line respectively in the Fig. 3, there we show also the disk contribution (dotted line) as a thermal component with temperature of  $kT=1$  eV in the quasar rest frame, no any additional reflection component has been included. The input parameters for our model are reported in the Table 2. We assume that the electrons distribution is a power-law,  $N \propto \gamma^{-p}$  in the range  $\gamma_{\text{min}} - \gamma_{\text{max}}$ . The photons in the external field of the BLR are also up-scattered from the relativistic electrons in the jet. Assuming that the BLR reprocesses a fraction of the disk luminosity (fixed at the level of the optical-UV observed in the SED) that is about 0.1 (Maraschi & Tavecchio 2003), the energy density in the observer frame is  $U_{\text{BLR}} = L_{\text{BLR}}/4\pi c R_{\text{BLR}}^2$  then the contribution of the inverse Compton to the SED is  $L_{\text{EC}} = 4/3 \sigma_T c N(\gamma) \gamma^2 U_{\text{BLR}} d\gamma = 8 \times 10^{48} R_{\text{BLR},17}^2 \text{ erg cm}^{-3} \text{ s}^{-1}$ , where  $R_{\text{BLR},17}$  is the BLR extension in unit of  $10^{17}$  cm and assuming that the Doppler factor of the jet  $\delta = \Gamma$ . Assuming for 4C04.42  $R_{\text{BLR},17} = 5 \times 10^{17}$  cm, and with the emitting volume given by  $V = 4/3 \pi R^3$ ,  $L_{\text{EC}} = 3 \times 10^{47} \text{ erg s}^{-1}$ , the value we measured in the SED. The observed soft X-ray excess could be due to bulk Compton of "cold" shell of plasma moving in the jet on the external BLR photon field (Celotti et al. 2006). The peak of this component is expected at the frequency of  $\nu_{\text{BC}} = \Gamma^2 \nu_{\text{BLR}}/(1+z) \sim 1$  keV, with  $\nu_{\text{BLR}}$  the peak frequency of the target photons. The luminosity  $L_{\text{BC}}$  is determined by the relative normalizations of the density numbers of the cold and relativistic electrons.

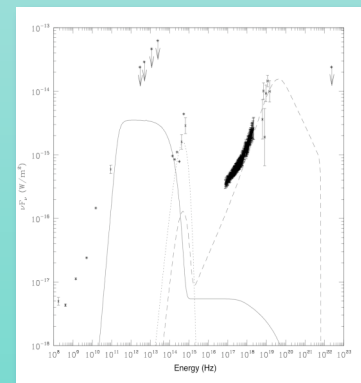


Fig 3. SED: data with SSC+EC model

Table 2. SED model parameters

B (Gauss)	R (cm)	$\delta$	N ( $\text{cm}^{-3}$ )	$\gamma_{\text{min}}/\gamma_{\text{max}}$	p	$L_{\text{BLR}}$ ( $\text{erg s}^{-1}$ )	$kT_{\text{BB}}$ (eV)
2	$3 \times 10^{16}$	20	$10^4$	1/1000	3	$2 \times 10^{45}$	1

## References

- Bird, A., Malizia, A., Bazzano, A., et al. 2007, ApJS, 170, 175
- Cappi, M., et al. 1997, ApJ 478, 492
- Celotti, A., Ghisellini, G., Fabian, A.C. 2006, MNRAS, 375,
- De Rosa A., Bassani L., Ubertini P. et al. 2008, MNRAS Letter in press. arXiv:0805.1941
- Dermer, C. D., & Schlickeiser, R. 1993, ApJ, 416, 458
- Fiore, F., Elvis, M., Giommi, P., Padovani, P. 1998, ApJ, 492, 79
- Fossati, G., Maraschi, L., Celotti, A., Comastri, A., Ghisellini, G. 1998, MNRAS, 299, 433
- Ghisellini, G., Celotti, A., Fossati, G., Maraschi, L., Comastri, A. 1998, MNRAS, 301, 451
- Maraschi, L. & Tavecchio, F. 2003, ApJ, 593, 667
- Kataoka, J., Madejski, G., Sikora, M., et al. 2007, ApJ, accepted, arXiv:0709.1528
- Sambruna, R.M., Gliozzi, M., Tavecchio, F., Maraschi, L., Foschini, L. 2006, ApJ, 2006, 652, 146
- Yuan W., Fabian A.C., Worsley M.A., McMahon R., 2006, MNRAS, 368, 985